Magnetic and electronic properties of ordered double-perovskite La_2VMnO_6 thin films

S. Chakraverty,[1,*] K. Yoshimatsu,[2] Y. Kozuka,[3] H. Kumigashira,[2] M. Oshima,[2] T. Makino,[1] A. Ohtomo,[4] and M. Kawasaki[1,3,5]

[1]*Cross-Correlated Materials Research Group (CERG) and Cross-correlated Materials Research Group (CMRG), RIKEN Advanced Science Institute, Wako 351-0198, Japan*

[2]*Department of Applied Chemistry, University of Tokyo, Tokyo 113-8656, Japan*

[3]*Quantum-Phase Electronics Center and Department of Applied Physics, University of Tokyo, Tokyo 113-8656, Japan*

[4]*Department of Applied Chemistry, Tokyo Institute of Technology, Tokyo 152-8552, Japan*

[5]*CREST, Japan Science and Technology Agency, Tokyo 102-0075, Japan*

(Received 3 August 2011; published 19 October 2011)

We report the stabilization of the *B*-site-ordered phase of epitaxial La_2VMnO_6 double-perovskite films grown by pulsed-laser deposition. Previous theoretical calculation predicted the possibility of realizing a spin-compensated half-metallic state in this system with an Mn^{3+} ion at a low spin state. In contrast, our magnetic measurements suggest that the system in ordered phase is ferrimagnetic with Mn^{3+} at a high spin state. Synchrotron radiation photoemission measurement indicates that the electronic ground state of this material is insulating: occupied Mn 3*d* t_{2g}, Mn 3*d* e_g, and V 3*d* t_{2g} states are located far from the Fermi level. The optical band gap is estimated to be about 0.9 eV, which is similar to the charge transfer gap of $LaMnO_3$ based on the optical absorption spectra.

DOI: 10.1103/PhysRevB.84.132411 PACS number(s): 81.15.Fg, 75.47.Lx, 75.70.−i, 75.30.Et

Half-metallic antiferromagnets (HMAFM's) were proposed over a decade ago by van Leuken and de Groot.[1] These materials have attracted enormous attention in recent times as they offer a unique possibility of realizing an interesting state that has a large degree of spin polarization of conduction electrons but vanishing macroscopic magnetic moment. Unlike a conventional antiferromagnet, in a HMAFM the nullification of magnetic moment occurs between antiparallel spins of the same magnitude, residing on different ions of distinct symmetry, and as a result a perceptible exchange splitting between the up- and down-spin channels is observed. Such materials can be potential candidates for a new generation of spin-based devices. It had also been predicted that these materials may offer an exotic superconducting state, namely, single spin superconductivity.[2] A large number of systems, e.g., metal alloys,[3,4] metal pnictides,[5] etc., have been theoretically predicted to be possible HMAFM candidates, but none of them have been experimentally realized so far.

In this respect, double-perovskite materials ($AB'B''O_6$) have turned out to be one of the popular searching grounds[6–9] because of the variety of choices in the B', B'' cations to achieve desired properties. However, the realization of double perovskites with highly ordered phase is restricted experimentally, which makes experimental verification of the proposed materials difficult. One of the potential double perovskites is La_2VMnO_6, which had been predicted theoretically to be a HMAFM system based on band calculation using the local spin-density approximation, assuming the low spin state of Mn^{3+} ion.[6] Some experimental studies have already been reported on the bulk disordered phase of this material, but a clear conclusion is still missing because of *B*-site disorder in the material.[10]

In this Brief Report, we report the stabilization of ordered double-perovskite La_2VMnO_6 (LVMO) in thin-film form using the pulsed-laser deposition (PLD) technique, grown along the (111) direction on $SrTiO_3$ (STO) substrate. A high degree of ordering can be achieved within a narrow window of growth condition. Magnetic measurements suggest ferrimagnetic behavior arising from uncompensated magnetic moments of V and Mn ions. Saturation magnetization is $\sim 2\ \mu_B$/formula unit (f.u.) at 5 K, suggesting a high spin state of the Mn^{3+} ion. The existence of Mn^{3+} ions with high spin states is further confirmed by photoemission measurement. The resonant photoemission technique indicates that the ground state of the LVMO thin film is insulating. The optical absorption spectrum shows the existence of an optical gap around 0.9 eV, similar to that of $LaMnO_3$.

Approximately 50-nm-thick LVMO films were grown on atomically flat (111) STO substrates using an ultrahigh vacuum PLD system with KrF excimer laser pulses (5 Hz) focused on a target (a La_2VMnO_6 disordered ceramic tablet with the single phase of orthorhombic structure, 99.99% purity) at a fluence of 1.1 J/cm^2 (laser spot area 0.35 × 0.10 cm^2).[11] After the growth, samples were quenched to room temperature, keeping oxygen partial pressure (P_{O_2}) constant. The film composition was analyzed for those grown on (001) MgO substrates under the same conditions by using a scanning electron microscopy equipped with an electron probe microanalyzer. The composition of cations was confirmed to be identical to that of the target regardless of growth condition. To characterize the crystal structure, x-ray diffraction (XRD) patterns were obtained by four-circle XRD (X'pert MRD, PANalytical) with CuK_α radiation ($\lambda = 1.5418$ Å). Magnetic properties were measured in a magnetic property measurement system operated in "reciprocating sample option" mode. Nonmagnetic tools were used to cut and handle the samples for avoiding possible magnetic contamination. Photoemission measurements were performed at an undulator beamline of BL2C in Photon Factory, KEK. All spectra were recorded using an SES-2002 electron energy analyzer with an energy resolution of about 150 meV. The Fermi level (E_F) of the sample was referred to that of gold. The optical spectrum was measured at room temperature in the energy range from 0.5 to 2 eV to evaluate the band gap.

Strong growth-condition dependence of the degree of ordering (defined as the intensity ratio of 111-superlattice reflection to 222-fundamental reflection) has been found as summarized in Fig. 1(a). Highly ordered films were reproducibly obtained

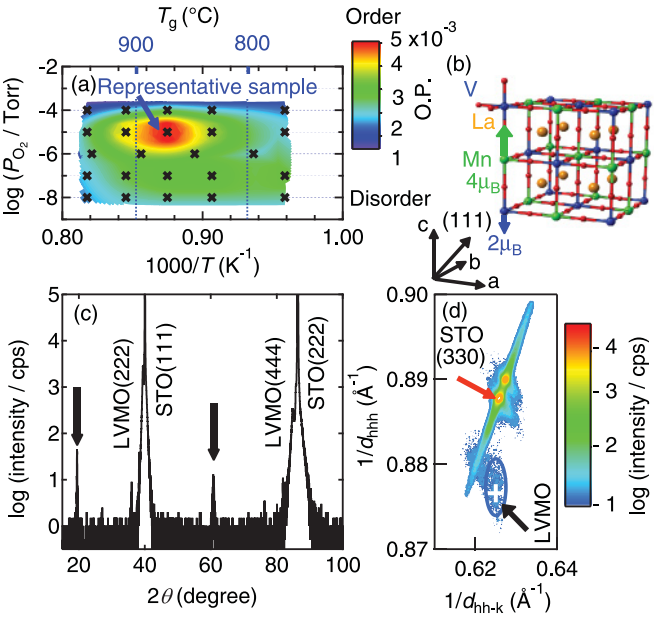

FIG. 1. (Color online) (a) Mapping of degree of order in B-site ions as a function of the oxygen partial pressure (P_{O_2}) and growth temperature (T_g) for the various samples with single-phase perovskite structure. Color code indicates the order parameter (O.P.), defined as the ratio of 111-superlattice reflection intensity to that of 222-fundamental reflection. Crosses (x) indicate the growth conditions used for the optimization. The representative sample having the highest O.P. has been used for all other measurements. (b) The schematic crystal structure of ordered LVMO sample. The possible ferrimagnetic spin structure with Mn at high spin state is also shown. (c) $\theta - 2\theta$ scan of x-ray-diffraction pattern of the representative sample. The superlattice peaks coming due to ordering are marked with arrows. (d) Reciprocal space map taken around 330 STO reflections.

at growth temperature (T_g) = 880 °C and $P_{O_2} = 1 \times 10^{-5}$ Torr [marked as representative sample in Fig. 1(a): this sample has been used for all subsequent experiments]. A schematic crystal structure of ordered LVMO is shown in Fig. 1(b). Figure 1(c) shows the $\theta - 2\theta$ plot of the representative sample. Superlattice reflections [as indicated in Fig. 1(c) by arrows] appear along the out of plane (hhh) axis with h being an odd integer, confirming the formation of a well-ordered phase of LVMO thin film. Figure 1(d) shows the reciprocal space map of the sample taken around (330) STO reflections; the film peak is marked (+) in the figure, which shows that the LVMO film is locked in plan with STO substrate. A rough estimation from the ratio of 111-superlattice to 222-fundamental peak intensities shows that the representative sample is more than 80% B-site order.[12]

The theoretical prediction of half-metallicity and spin compensation was based on the assumption that the lattice parameter of the fundamental perovskite unit cell of the material was 3.89 Å.[6] Thus, it will be important to determine lattice parameters for our samples. Judging from the position of asymmetric reflections, we have concluded that the film investigated in this study was pseudomorphically grown on (111) STO, as seen in Fig. 1(d). From this fact, the average lattice parameter (a_{av}) is deduced through $a_{av} = V_{av}^{1/3}$, where V_{av} is the volume of the LVMO unit cell, which satisfies

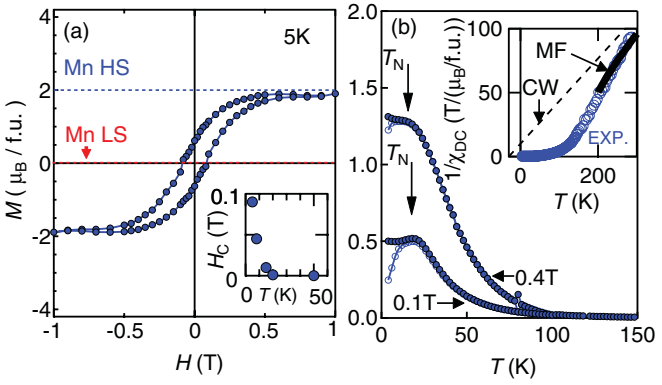

FIG. 2. (Color online) (a) Magnetization (M) measured at 5 K as a function of applied magnetic field (H). The ideal values of the magnetization with Mn at high spin (HS) and low spin (LS) states are also indicated by dashed lines. Inset shows the coercive field (H_C) as a function of temperature. (b) The field-cooled (•) and zero-field-cooled (○) magnetization as a function of temperature taken with 0.1-T (lower curve) and 0.4-T applied magnetic fields. The Néel temperature (T_N) has been marked with arrows. Inset shows the inverse of DC susceptibility ($1/\chi_{DC}$) as a function of temperature (○). Fitting with molecular field theory (MF) and corresponding high-temperature Curie-Weiss limit (CW) plot is also shown.

the condition $V_{av} = 12\sqrt{3}\times(d_{11-2})^2\times d_{111}$, where d_{111} is the measured value for LVMO and d_{11-2} is a constant for STO. The lattice parameter estimated from this for our present LVMO sample is 3.919 Å, deviating only 0.75% larger than the theoretically assumed value.

Using a SQUID (superconducting quantum interference devices) magnetometer, magnetization vs applied magnetic field and temperature were measured for the representative sample. As shown in Fig. 2(a), the in-plane magnetization loop taken at 5 K traced well-defined magnetic hysteresis. Figure 2(a) shows that the magnetization saturates at an 1-T field. The saturation magnetization (M_s) at 1 T was around 1.9 μ_B/f.u. with an error arising from inaccuracy of the film volume (±0.15 μ_B/f.u.). The magnitude of M_s is consistent with antiferromagnetic ordering of local spin moment with Mn^{3+} at high spin state ($V^{3+}Mn^{3+}$: $3d_{\downarrow}{}^2 3d_{\uparrow}{}^4 \Rightarrow 2.0\,\mu_B$/f.u.). The ideal values of the magnetization in high- and low-spin states of Mn^{3+} are marked in Fig. 2(a) with dotted lines. Field-cooled (FC) and zero-field-cooled (ZFC) magnetization measurements have been carried out at a different applied field (H), as shown in Fig. 2(b). A bifurcation in FC and ZFC curves followed by a hump at around 21 K in the ZFC curve had been observed. This bifurcation may be confused with a similar observation in spin-glass magnets. To clarify, we have performed FC-ZFC measurements at different magnetic fields as shown in Fig. 2(b). The position of the peak in the FC-ZFC curve was independent of H. It is also worth noting that the bifurcation between FC and ZFC became vanishingly small when the measurement was carried out under an H = 0.4 T magnetic field, a field greater than the coercive field (around 0.1 T) of the system. In the inset of Fig. 2(a), the coercive field as a function of temperature is plotted. The coercivity vanishes at around 20 K. These observations suggest that the bifurcation is an effect of coercivity. The peak is associated with the antiferromagnetic ordering temperature

of the sample. The Néel temperature (T_N) as deduced from the peak of the FC-ZFC curve is 21 K. The inverse of DC susceptibility ($1/\chi_{DC}$) as a function of temperature (○) is shown in the inset of Fig. 2(b). This curve is fitted in the temperature range of 200 to 300 K with the molecular field theory formula for ferrimagnetic materials, and corresponding parameters had been used to extract the Curie-Weiss (CW) temperature. Curie-Weiss temperature estimated from the intercept of the CW plot is −30 K, which agrees quite well with the T_N measured from FC-ZFC curve.

In order to verify the valence state and the electronic structures on the LVMO thin film, we have performed synchrotron radiation photoemission spectroscopy. Figure 3 shows valence band and resonant valence band spectra of the LVMO thin film. In the valence band spectra, the prominent structures located from 9 eV to 4 eV are derived from the O 2*p* states. Other features labeled *A*, *B*, and *C* near E_F may be derived from Mn 3*d* and/or V 3*d* states. On the other hand, there is no density of states at E_F, indicating the insulating ground state of the LVMO thin film. In order to assign their states, the Mn 2*p*-3*d* and V 2*p*-3*d* resonant spectra were measured. In the V 2*p*-3*d* resonant spectrum, feature *C* located at about 1.2 eV below E_F is resonantly enhanced, suggesting the V 3*d* t_{2g} nature of the states. On the other hand, in the Mn 2*p*-3*d* resonant spectrum, features *A* and *B* were resonantly enhanced, suggesting that they were derived from the Mn 3*d* states. In comparison to the cluster model calculation,[15] features *A* and *B* were assigned to the Mn 3*d* t_{2g} and e_g states, respectively. The accommodation of electrons in Mn 3*d* e_g states presents two important pieces of information: (i) Mn ions have high spin states, and (ii) the valence of Mn ions is not greater than 3+. We also investigated the valence of Mn ions from the Mn *L*-edge x-ray absorption spectra (not shown), and confirmed that Mn ions were mainly 3+ states. As a result, the valence of V ions is estimated to be 3+ because the sum of the valence in transition metal ions should be 6+. O 2*p* derived states are mainly located below 4 eV in the valence band. Fully occupied $t_{2g\uparrow}$ and partially occupied $e_{g\uparrow}$ derived states of Mn^{3+} are located at about 3.0 and 1.7 eV below E_F, respectively. On the other hand, V ions also had 3+ states, and partially occupied $t_{2g\downarrow}$ derived states are located about 1.2 eV below E_F. The V 3*d* $t_{2g\downarrow}$ states are isolated from E_F, indicating that the electronic ground state of the LVMO thin film is insulating. The energy diagram and ground state of the LVMO thin film revealed in this experiment are not in agreement with those predicted from the band calculation.[6]

Having established the basic spin and electronic structures, it is interesting to compare the optical spectrum of LVMO with those of component perovskites, namely, charge transfer (CT) insulator $LaMnO_3$ and Mott-Hubbard insulator $LaVO_3$.[18] Since the Mn and V ions couple antiferromagnetically in LVMO and the major spin bands are partially occupied on both sites, we can rule out the interionic transfer between Mn and V ions (the spin-forbidden selection rule). Therefore, this comparison will be rather meaningful. The gap energies of $LaMnO_3$ and $LaVO_3$ are scaled with on-site correlation energy of the respective ions (Mn and V). In the case of ideally ordered double perovskites, there will be no nearest neighboring pair of the same ions; thus it is not straightforward to predict the gap energy in LVMO.

Figure 4 shows the optical absorption spectrum of the LVMO thin film taken at room temperature. A plausible energy diagram has also been drawn based on the result of photoemission and optical spectroscopies in the inset of Fig. 4.

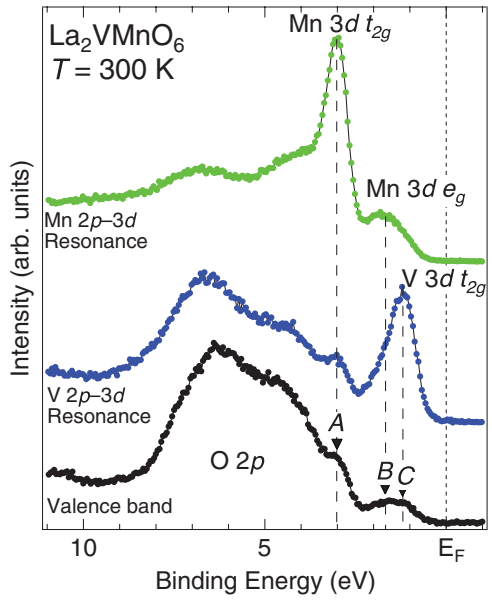

FIG. 3. (Color online) Valence band (bottom), V 2*p*-3*d* (middle), and Mn 2*p*-3*d* (top) resonant spectra in the LVMO thin film. The valence band spectra were taken at a photon energy of 600 eV to obtain the highest photon flux in the beam line. V 2*p*-3*d* and Mn 2*p*-3*d* resonant spectra were taken at the photon energy of 518 eV (Ref. 13) and 644 eV (Ref. 14) determined by V and Mn *L*-edge x-ray-absorption spectra, respectively.

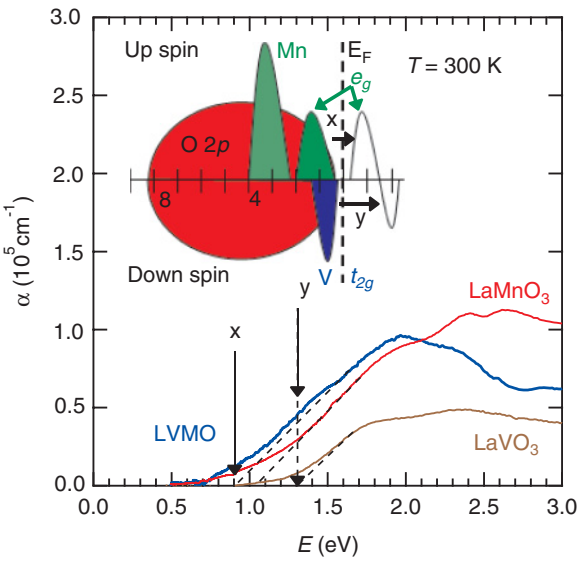

FIG. 4. (Color online) Absorption spectrum of LVMO thin film taken at room temperature. The optical spectra of $LaMnO_3$ (Ref. 16) and $LaVO_3$ (Ref. 17) are also shown for comparison. Inset shows plausible energy diagram of LVMO based on the result of photoemission and optical spectra. The arrows *x* and *y* indicate the absorption bands corresponding to the optical transitions denoted in the inset. The minimal optical gap energies were determined by the linear interpolation method, as shown with dashed lines.

The lowest optical gap is evaluated to be approximately 0.9 eV through the linear interpolation method.[19] The threshold energy, corresponding to the intercept of the abscissa with the dashed line of the absorption band (x), is similar to but slightly lower than the CT gap (O $2p \rightarrow$ Mn $3d$) energy (1.0 eV) of $LaMnO_3$.[19] This is possibly due to CT gap narrowing of the LVMO associated with the crystal structure change in this double perovskite. Another feature appears around 1.3 eV (as marked by y), which is energetically quite similar to the Mott-type gap energy of $LaVO_3$.[20] It is worth noting that the absorption substructures at E $\simeq$2.4 eV are weakened in the LVMO spectrum. This structure, coming from the momentum dependence of the electron energy band is known as "subpeak structures".[21] The quench of the absorption at $E \simeq$ 2.4 eV may be related to the double-perovskite modification effect of the dispersion relation. Further theoretical attention should be paid for the better understanding of the electronic band structure of this material, taking into account possible orbital ordering.

In conclusion, we have stabilized highly ordered 111-oriented La_2VMnO_6 double perovskite in thin-film form by using pulsed-laser deposition on STO (111) substrate. The lattice parameter of the film is 0.75% larger than that assumed for theoretical calculation. The ground state of this material in ordered phase is ferrimagnetic with Mn^{3+} at a high spin state, as confirmed by magnetic as well as photoemission measurements. Photoemission measurement shows that this material is insulating. The energy diagram of this material is that Mn $3d\ t_{2g}$, Mn $3d\ e_g$, and V $3d\ t_{2g}$ states are located far from E_F determined by the resonant photoemission technique. The optical band gap is estimated to be about 0.9 eV. A plausible energy diagram has been drawn based on the result of photoemission and optical spectroscopies.

S.C. is grateful to Y. Tokura for illuminating discussion on optical spectroscopy. A.O. is supported by the GCOE program (Chemistry), Tokyo Institute of Technology, and JSPS. This work was partly supported by JSPS through its Funding Program for World-Leading Innovation R&D on Science and Technology (FIRST) program.

*suvankar.chakraverty@riken.jp

[1] H. van Leuken and R. A. de Groot, Phys. Rev. Lett. **74**, 1171 (1995).
[2] R. E. Rudd and W. E. Pickett, Phys. Rev. B **57**, 557 (1998).
[3] H. Luo, L. Ma, Z. Zhu, G. Wu, H. Liu, J. Qu, and Y. Li, Physica B **403**, 1797 (2008).
[4] J. I. Lee, B. Bialek, and M. Y. Kim, J. Appl. Phys. **105**, 07E508 (2009).
[5] N. H. Long, M. Ogura, and H. Akai, J. Phys. Condens. Matter **21**, 064241(2009).
[6] W. E. Pickett, Phys. Rev. B **57**, 10613 (1998).
[7] K.-W. Lee and W. E. Pickett, Phys. Rev. B **77**, 115101 (2008).
[8] J. H. Park, S. K. Kwon, and B. I. Min, Phys. Rev. B **65**, 174401 (2002).
[9] Y. K. Wang and G. Y. Guo, Phys. Rev. B **73**, 064424 (2006).
[10] J. Androulakis, N. Katsarakis, and J. Giapintzakis, Solid State Commun. **124**, 77 (2002).
[11] S. Chakraverty, A. Ohtomo, M. Okude, K. Ueno, and M. Kawasaki, Cryst. Growth Des. **10**, 1725 (2010).
[12] S. Chakraverty, A. Ohtomo, D. Okuyama, M. Saito, M. Okude, R. Kumai, T. Arima, Y. Tokura, S. Tsukimoto, Y. Ikuhara, and M. Kawasaki, Phys. Rev. B **84**, 064436 (2011).
[13] R. Eguchi, M. Taguchi, M. Matsunami, K. Horiba, K. Yamamoto, Y. Ishida, A. Chainai, Y. Takata, M. Yabashi, D. Miwa, Y. Nishino, K. Tamasaku, T. Ishikawa, Y. Senba, H. Ohashi, Y. Muraoka, Z. Hiroi, and S. Shin, Phys. Rev. B **78**, 075115 (2008).
[14] K. Horiba, A. Chikamatsu, H. Kumigashira, M. Oshima, N. Nakagawa, M. Lippmaa, K. Ono, M. Kawasaki, and H. Koinuma, Phys. Rev. B **71**, 155420 (2005).
[15] T. Saitoh, A. E. Bocquet, T. Mizokawa, H. Namatame, A. Fujimori, M. Abbate, Y. Takeda, and M. Takano, Phys. Rev. B **51**, 13942 (1995).
[16] S. Miyasaka, Y. Okimoto, and Y. Tokura, J. Phys. Soc. Jpn. **71**, 2086 (2002)
[17] M. Nakamura, A. Sawa, J. Fujioka, M. Kawasaki, and Y. Tokura, Phys. Rev. B **82**, 201101 (2010).
[18] M. Imada, A. Fujimori, and Y. Tokura, Rev. Mod. Phys. **70**, 1039 (1998).
[19] T. Arima, Y. Tokura, and J. B. Torrance, Phys. Rev. B **48**, 17006 (1993).
[20] T. Arima and Y. Tokura, J. Phys. Soc. Jpn. **64**, 2488 (1995).
[21] M. W. Kim, P. Murugavel, S. Parashar, J. S. Lee, and T. W. Noh, New J. Phys. **6**, 156 (2004).